Cell Insight 3 (2024) 100186

Contents lists available at ScienceDirect

Cell Insight

journal homepage: www.journals.elsevier.com/cell-insight

Research Article

Deacetylation of GLUD1 maintains the survival of lung adenocarcinoma cells under glucose starvation by inhibiting autophagic cell death

Qifan Hu [a,b,c,1], Longhua Sun [a,1], Zhujun Cheng [d], Lei Wang [e], Xiaorui Wan [a], Jing Xu [e], Junyao Cheng [a], Zuorui Wang [e], Yi Yuan [f], Keru Wang [f], Tianyu Han [a,g,*]

[a] Jiangxi Provincial Key Laboratory of Respirtory Diseases, Jiangxi Institute of Respiratory Diseases, The Department of Respiratory and Critical Care Medicine, The First Affiliated Hospital, Jiangxi Medical College, Nanchang University, Nanchang, 330006, Jiangxi, China
[b] Department of Thoracic Surgery, The First Affiliated Hospital of Nanchang University, Nanchang, 330006, Jiangxi, China
[c] Postdoctoral Innovation Practice Base, The First Affiliated Hospital, Jiangxi Medical College, Nanchang University, Nanchang, 330006, Jiangxi, China
[d] Department of Burn, The First Affiliated Hospital of Nanchang University, Nanchang, 330006, Jiangxi, China
[e] School of Basic Medical Sciences, Nanchang University, Nanchang, 330031, Jiangxi, China
[f] School of Huankui Academy, Nanchang University, Nanchang, 330031, Jiangxi, China
[g] China-Japan Friendship Jiangxi Hospital, National Regional Center for Respiratory Medicine, Nanchang, 330200, Jiangxi, China

HIGHLIGHTS

- GLUD1 maintains the survival of lung adenocarcinoma cells under glucose starvation.
- GLUD1 de-acetylation on Lys84 promotes the highly active hexamer formation.
- Deacetylation of GLUD1 induces the cytoplasmic localization and the interaction with cytoplasmic glutaminase KGA.
- Cytoplasmic GLUD1 interacts with p62 and prevents p62 body formation.

GRAPHICAL ABSTRACT

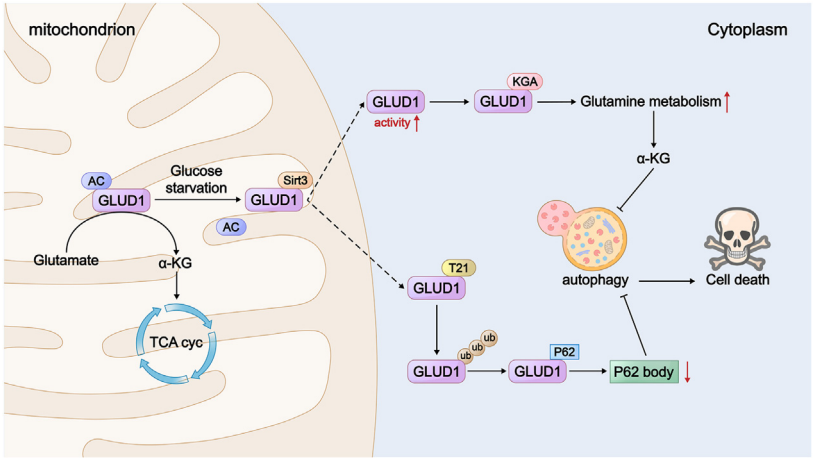

ABSTRACT

Enhanced glutamine catabolism is one of the main metabolic features of cancer, providing energy and intermediate metabolites for cancer progression. However, the functions of glutamine catabolism in cancer under nutrient deprivation need to be further clarified. Here, we discovered that deacetylation of glutamate dehydrogenase 1 (GLUD1), one of the key enzymes in glutamine catabolism, maintains the survival of lung adenocarcinoma (LUAD) cells under glucose starvation by inhibiting autophagic cell death. We found that glucose starvation increased GLUD1 activity by reducing its acetylation on Lys84 and promoted its active hexamer formation. Besides, deacetylation of GLUD1 induced its cytoplasmic localization, where GLUD1 was ubiquitinated in K63-linkage by TRIM21, leading to the binding of GLUD1 with cytoplasmic glutaminase KGA. These two effects enhanced glutamine metabolism both in mitochondria and cytoplasm, increased the production of alpha-

* Corresponding author. Jiangxi Provincial Key Laboratory of Respirtory Diseases, Jiangxi Institute of Respiratory Diseases, The Department of Respiratory and Critical Care Medicine, The First Affiliated Hospital, Jiangxi Medical College, Nanchang University, Nanchang, 330006, Jiangxi, China.
E-mail address: hantianyu87@163.com (T. Han).
[1] These authors contributed equally to this work.

https://doi.org/10.1016/j.cellin.2024.100186
Received 20 December 2023; Received in revised form 12 July 2024; Accepted 14 July 2024
Available online 16 July 2024

ketoglutarate (α-KG). Meanwhile, cytoplasmic GLUD1 also interacted with p62 and prevented its acetylation, leading to the inhibition of p62 body formation. All these effects blocked autophagic cell death of LUAD cells under glucose starvation. Taken together, our results reveal a novel function of GLUD1 under glucose deprivation in LUAD cells and provide new insights into the functions of glutamine catabolism during cancer progression.

1. Introduction

The rapid proliferation of cancer cells requires a great amount of energy and nutrients (Faubert et al., 2020; Grasmann et al., 2019). However, the highly nutritional needs of cancer cells are often not adequately supplied. Although angiogenesis is activated early in cancer progression, the newly formed network of blood vessels is abnormal, with leaky vessels and irregular, fluctuating blood flow. Particularly, glucose deprivation appears to be common due to its high consumption rate of cancer cells. Researchers also found that glucose concentrations were lower in tumors than in corresponding normal tissues (Duarte et al., 2010; Hirayama et al., 2009; Rocha et al., 2010, 2015; Urasaki et al., 2012; Wang et al., 2013; Ziebart et al., 2011). The mechanisms underlying cancer cell adaptation to such a fluctuating nutrient supply are under intense investigation, since they may reveal specific vulnerabilities of cancer cells.

Metabolic reprogramming is one of the hallmarks of cancer and enhanced glutamine consumption is an important aspect. Glutamine is converted into ammonium and glutamate through glutaminase (GLS), then glutamate was converted into alpha-ketoglutarate (α-KG) by glutamate dehydrogenase 1 (GLUD1), therefore entering the TCA cycle to generate intermediates and energy for the synthesis of biological macromolecules (Hu et al., 2023a). Our previous studies demonstrated that the activity of GAC (kidney-type glutaminase) was regulated by phosphorylation in lung adenocarcinoma (LUAD)(Han et al., 2018). However, as another important enzyme in glutamine metabolism, the regulatory mechanisms for GLUD1 in LUAD were not so clear. In human body, glutamate dehydrogenase has two subtypes: GLUD1 and GLUD2. GLUD1 has a higher activity and less sensitivity to the activation of ADP compare with GLUD2 (Liu et al., 2020; Paul & Ghosh, 2015). Researchers found that GLUD1 provides a metabolic advantage to cancer cells through regulating carbon and nitrogen metabolism (Chu et al., 2021; Luan et al., 2018; Wei et al., 2021; Zhang et al., 2021). However, little is known about the function and regulatory mechanism for GLUD1 in cancer progression under nutrient deprivation.

Post-translational modifications (PTM) such as acetylation, succinylation and ubiquitination, expand the functional diversity of the substrate proteins by affecting its activity or expression (Hirschey & Zhao, 2015). Acetylation is a process that covalently binding of acetyl groups to the lysine residues of substrate proteins to affect the function of the proteins (Verdin & Ott, 2015). In mitochondrial, acetylation is one of the key modifications that regulates the proper functions of mitochondrial proteins (Carrico et al., 2018; Liu et al., 2018). In this study, we found that GLUD1-mediated glutamine metabolism could maintain the survival of LUAD cells by inhibiting autophagic cell death under glucose starvation (GS). The activity of GLUD1 significantly increased under glucose deprivation and its activity was regulated by acetylation. We further discovered that GLUD1-K84 acetylation was the key acetylation site under GS, and SIRT3 deacetylated GLUD1 on K84 and increased its enzymatic activity by promoting its hexamer formation. Intriguing, GS-mediated deacetylation of GLUD1 promoted its cytoplasmic localization followed by K63-linked ubiquitination catalyzed by TRIM21, this led to the formation of GLUD1-KGA complex and further enhanced cytoplasmic glutamine metabolism. Moreover, cytoplasmic GLUD1 could also interact with p62 and blocking the formation of p62 bodies. Thus, our study elucidates a new role of GLUD1 in maintain the survival of LUAD cells under GS, which further deepens people's understanding of glutamine metabolism in cancer and provides a theoretical basis for developing anti-tumor drugs.

2. Results

2.1. The expression of GLUD1 maintains the survival of LUAD cells under glucose starvation

Enhanced glutamine catabolism is regarded as an important feature of cancer metabolic reprogramming, which provides survival advantages for cancer development via providing energy and macromolecular precursors required for biosynthesis (Hanahan & Weinberg, 2011; Liang et al., 1999). However, the functions of glutamine catabolism under nutrient deprivation needed to be further clarified. To investigate the changes of glutamine catabolism under glucose starvation (GS), we detected the content of metabolites produced by glutamine catabolism. Fig. 1 A-C showed that the content of glutamate was significantly decreased, while ammonia (NH4) and α-ketoglutarate (α-KG) were up-regulated under GS. These results suggested that glutamine catabolism was enhanced under GS. To further explore how GS affected the glutamine catabolism, we tested the expression of GLUD1 and glutaminase (GAC), the key enzymes in glutamine catabolism. The results showed that glucose deprivation did not affect the expression of GAC and GLUD1 (Fig. 1D and E). Then, the enzymatic activities of GLUD1 and GAC were detected. The results showed that GS treatment increased GLUD1 activity but not GAC activity in A549 and H1299 cells (Fig. 1F and G). These results indicated that glucose starvation elevated glutamine metabolism by upregulating the activity of GLUD1.

We then constructed stable cell lines with GLUD1 overexpression or knockout to further explore its function under GS (Figs. S1A and B). Upon exposure to GS, cells stably overexpressing GLUD1, but not wild-type A549 cells, were able to maintain the survival state (Fig. 1H). However, cells with GLUD1 knockout died more rapidly than wild-type cells under GS (Fig. 1I). Then, cell viability assays were performed under GS. We found that cells with GLUD1 overexpression had better viability than wild-type A549 cells, while cells with GLUD1 knockout showed worse viability than wild-type A549 cells (Fig. 1J and K). These results were further determined in LUAD organoids. 2-Deoxy-D-glucose (2-DG), a glucose analogue, was used to inhibit the glucose metabolism to mimic glucose starvation. The GLUD1 inhibitor R162 was used to inhibit GLUD1 activity. We found that 2-DG inhibited the growth of LUAD organoid and R162 treatment further enhanced the inhibitory effect (Fig. 1L). Collectively, these data suggest that GLUD1 maintains the survival of LUAD cells under GS.

2.2. GLUD1 inhibits autophagic cell death under glucose starvation by enhancing glutamine metabolism

We next explored the mechanism for GLUD1 in maintaining cell survival under GS. Autophagy can be induced under glucose starvation and we constructed H1299 stable cell line overexpressing GFP-LC3 to explore the formation of autophagosomes under GS. The number of autophagosomes significantly increased following GS (Fig. 2A). Autophagy is a double-edged sword which can both protect cells and kill cells in different physiological states. We then examined the function of GS-induced autophagy in LUAD cells. Beclin1 is a key autophagy related protein regulating the lipid kinase Vps34 by forming the Beclin1-Vps34-Vps15 complex (Liang et al., 1999). We then inhibited autophagy process by knocking down Beclin1 in A549 and H1299 cells and detected cell viability under GS. The results showed that inhibiting autophagy increased cell viability under GS (Fig. 2B), indicating that GS induced autophagic cell death. Previous study showed that GLUD1 knockdown

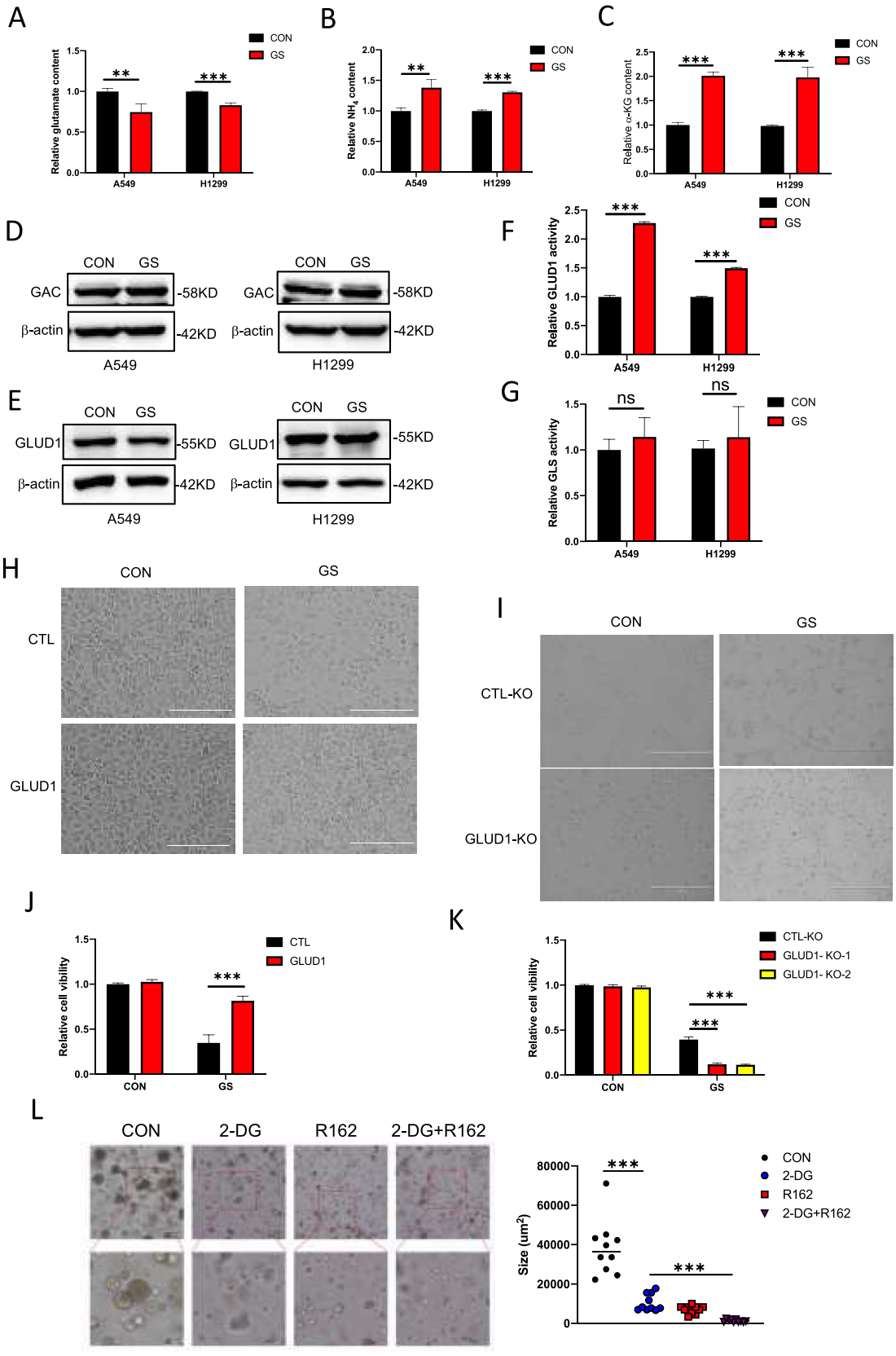

(caption on next page)

Fig. 1. Following GS, the up-regulate of GLUD1 activity promotes cell viability in LUAD cells. (A) The glutamate levels in A549 and H1299 cells under GS. Data represent the average of three independent experiments (mean ± SD). $^{**}P < 0.01$, $^{***}P < 0.001$. (B) The NH_4 levels in A549 and H1299 cells under GS. Data represent the average of three independent experiments (mean ± SD). $^{**}P < 0.01$, $^{***}P < 0.001$. (C) The level of α-KG in A549 and H1299 cells under GS. Data represent the average of three independent experiments (mean ± SD). $^{***}P < 0.001$. (D and E) A549 and H1299 cells were subjected to glucose starvation and Western blot was used to detect the expression of GAC (D) and GLUD1 (E). (F) The activity of GLUD1 in A549 and H1299 cells under GS was detected by Micro Glutamic Acid Dehydrogenase (GLUD) Assay Kit. Data represent the average of three independent experiments (mean ± SD). $^{***}P < 0.001$. (G) The activity of GLS in A549 and H1299 cells under GS was detected using Micro Glutaminase (GLS) Assay Kit. Data represent the average of three independent experiments (mean ± SD). ns > 0.05. (H and I) A549 cells (WT, stably expressing GLUD1 or stably knockout GLUD1) were treated with or without GS for 24 h. The changes of cell morphological was investigated (scale bar = 400 μm, magnification: × 100). (J and K) A549 cells (WT, stably expressing GLUD1 or stably knockout GLUD1) were treated with or without GS. Cell viability was determined by CCK-8 assay. Data represent the average of three independent experiments (mean ± SD). $^{***}P < 0.001$. (L) Representative images of the patient-derived organoids are shown (left-hand panel). The growth of the organoids was analyzed, and the size of organoids was calculated (right-hand panel). $^{***}P < 0.001$.

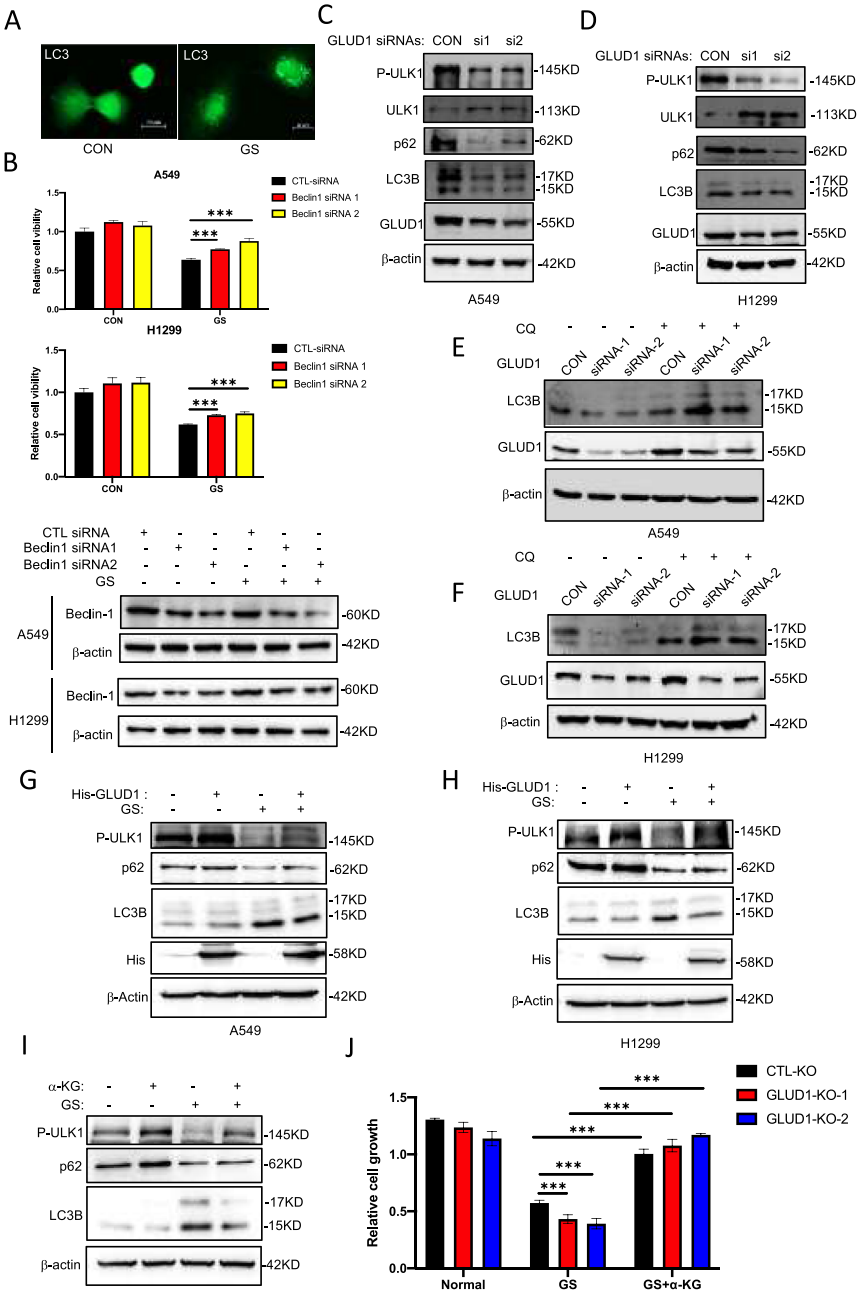

Fig. 2. GLUD1 promotes the viability of LUAD cells under GS via inhibiting of autophagy. (A) Stably overexpression of GFP-LC3 in H1299 cells were treated with or without GS for 24 h, the changes of autophagosomes was observed via immunofluorescence (scale bar: 20 μm, magnification: × 400). (B) Beclin1 siRNAs were transfected in A549 and H1299 cells treated with or without GS. Cell viability was determined by CCK-8 assay. The data represent the average of three independent experiments (mean ± SD). $^{***}P < 0.001$ (upper panel). The knockdown efficiencies of Beclin1 were detected by Western blot (bottom panel). (C and D) The GLUD1 siRNAs was transfected into A549 and H1299 cells, Western blot was used to detect the level of indicated proteins. (E and F) A549 and H1299 cells were knockdown GLUD1 through special siRNAs and treated with or without CQ, LC3B was detected by Western blot. (G and H) Stably overexpression of GLUD1 in A549 and H1299 cells was treated with or without GS. Indicated proteins was determined by Western blot. (I) A549 cells were treated with or without GS and added with or without α-KG (2.9 mM) for 24 h, Western blot was used to detect the level of indicated proteins. (J) A549 cells were treated with or without GS and added with or without α-KG (2.9 mM) for 24 h. Cell viability was determined using CCK-8. Data represent the average of three independent experiments (mean ± SD). $^{***}P < 0.001$.

induced autophagy in HeLa cells (Lorin et al., 2013). As GLUD1 expression maintained the survival of LUAD cells and its enzymatic activity significantly increased under GS, we speculated that GLUD1 protected cells from autophagic cell death by enhancing glutamine metabolism. To detect whether GLUD1 affect autophagy in LUAD cells, we knocked down GLUD1 and examined the expression of autophagy related proteins in LUAD cells. We found that GLUD1 knockdown decreased the expression of p62 and phospho-ULK1 (Ser757), but not ULK1. The expression of

both LC3B-I and II also decreased in cells with GLUD1 knockdown (Fig. 2C and D). We next detected autophagic flux in cells with GLUD1 knockdown by adding Chloroquine (CQ). We found that CQ treatment significantly increased the expression of LC3B-II in cells with GLUD1 knockdown, indicating that knocking down GLUD1 enhanced autophagic flux (Fig. 2E and F). These results demonstrated that GLUD1 knockdown induced autophagy in LUAD cells. We then determined whether GLUD1 inhibited autophagy in LUAD cells under GS. Fig. 2G and H demonstrated that GLUD1 overexpression inhibited GS-induced autophagy in A549 and H1299 cells, as shown by increased expression of p62 and phospho-ULK1 (Ser757) and decreased expression of LC3B-II. Alpha-ketoglutarate (α-KG) is a key downstream metabolite catalyzed by GLUD1. Previous studies have demonstrated that α-KG inhibited autophagy by activating mTOR (Yao et al., 2012). We next detected the effect of α-KG in GS-induced autophagy. Fig. 2I showed that α-KG treatment could block GS-induced autophagy. Addition of α-KG could recover cell viability under GS both in control and GLUD1 knockout cells (Fig. 2J). All these data indicate that GLUD1 rescues cells from GS-induced cell death by enhancing glutamine metabolism.

2.3. SIRT3 as a deacetylase, impairs the acetylation of GLUD1 and promotes its enzymatic activity

We then intended to clarify the mechanism for the enhanced activity of GLUD1 under glucose starvation. Previous study demonstrated that acetylation could regulate the enzymatic activity of GLUD1 (Li et al., 2019). As glucose-derived acetyl-CoA is the main substrate for acetylation, we next wanted to explore whether the increased activity of GLUD1 under GS was regulated by acetylation. Fig. 3A showed that GLUD1 was acetylated in A549 cells. We then detected whether glucose starvation affected GLUD1 acetylation. GS treatment down regulated the acetylation level of GLUD1 (Fig. 3B). These results demonstrated that GLUD1 was acetylated in LUAD cells and this acetylation was affected by GS. SIRT1, SIRT3, SIRT4 and SIRT5 are the deacetylases in mitochondria and regulates metabolic processes. We thus speculated if GLUD1 was deacetylated by SIRT family proteins in LUAD cells. For this purpose, we tested the interaction between SIRT proteins and GLUD1 by co-immunoprecipitation (co-IP). The result indicated that SIRT3 and SIRT4 interacted with GLUD1 (Fig. 3C). In A549 cells overexpressing SIRT3, the acetylated GLUD1 was lower than that in cells transfected with the others SIRTs (Fig. 3D). Conversely, in A549 cells with SIRT3 knockdown, we found that the acetylation level of GLUD1 increased (Fig. 3E). This result suggested that SIRT3 deacetylated GLUD1 in LUAD cells. We next investigated whether SIRT3 affected the expression or activity of GLUD1 protein. Overexpression of SIRT3 did not change the expression level of GLUD1 protein in LUAD cells (Fig. 3F). However, overexpression of SIRT3 increased the activity of GLUD1 under GS and normal conditions (Fig. 3G). In addition, SIRT3 promoted the production of α-KG in LUAD cells under GS and normal conditions (Fig. 3H). These data demonstrated that SIRT3, as a deacetylase, affected GLUD1 activity but not protein expression. Besides, we found that glucose starvation promoted the interaction between SIRT3 and GLUD1 (Fig. 3I). In order to investigate whether the activity of SIRT3 was enhanced under GS, we examined the changes in the acetylation levels of several classical SIRT3 substrates, including IDH2, MDH2 and SHMT2. Fig. 3 J-L showed that GS treatment down-regulated the acetylation levels of IDH2, MDH2 and SHMT2.

2.4. Acetylation on Lys84 of GLUD1 plays a key role in regulating its hexamer formation and enzymatic activity under glucose starvation

To investigate the key acetylation sites for GLUD1, we use PhosphoSitePlus and found that the K84, K480, K503, K527 and K548 were predicted as the putative acetylation sites (Fig. 4A). Then, we constructed the GLUD1 plasmids containing indicated mutations (K84R, K480R, K503R, K527R and K548R). We found that only $GLUD1^{K84R}$ abolished the decreased acetylation induced by SIRT3, and the acetylation of $GLUD1^{K84R}$ decreased compared with $GLUD1^{WT}$ (Fig. 4B and C). The acetylation of $GLUD1^{K84R}$ also did not change when treated with GS (Fig. 4D). These results indicated that K84 was the major acetylation site of GLUD1 regulated by GS. Next, we examined the effects of K84 acetylation on the functions of GLUD1. The enzymatic activity was detected, and the results indicated that the $GLUD1^{K84R}$ had a higher activity than $GLUD1^{WT}$ (Fig. 4E). Overexpression of $GLUD1^{K84R}$ in LUAD cells generated more α-KG than cells overexpressing $GLUD1^{WT}$ (Fig. 4F). Altogether, these data supported that the enzymatic activity of GLUD1 was regulated by acetylation and K84 was the major acetylation site of GLUD1 under GS. Moreover, SIRT3 did not affect the activity of $GLUD1^{K84R}$, further indicating that K84 was the key site for SIRT3 regulating the acetylation and activity of GLUD1 (Fig. 4G). Collectively, these data demonstrate that SIRT3 deacetylates GLUD1 on Lys84 and facilitates its enzymatic activity under GS and normal conditions.

Hexamer formation was essential for the high activity of GLUD1 (Haigis et al., 2006). We performed glutaraldehyde crosslink experiments to detect whether glucose starvation affected GLUD1 hexamer formation. We found that the hexamer status of GLUD1 was increased under GS (Fig. 4H). To explore how SIRT3 affected GLUD1 activity, we transfected SIRT3 in A549 cells stably overexpressing GLUD1 and glutaraldehyde crosslink experiments was performed. The GLUD1 hexamer was increased when cells were transfected with SIRT3 (Fig. 4I). Similarly, more hexamer was formed in cells transfected with $GLUD1^{K84R}$ than $GLUD^{WT}$ (Fig. 4J). These results suggest that SIRT3-mediated GLUD1-K84 deacetylation up-regulates its enzymatic activity by promoting the formation of hexamers.

2.5. The deprivation of glucose induces cytoplasmic localization of GLUD1

GLUD1 mainly localized in the mitochondria and researchers demonstrated that amino acid deprivation inhibited GLUD1 translocation from the cytoplasm into mitochondria in kidney renal clear cell carcinoma (KIRC) cells (Shao et al., 2021). We thus intended to explore whether glucose deprivation also affected the localization of GLUD1. In LUAD cells, we found that glucose starvation induced cytoplasmic localization of GLUD1 (Fig. 5A and B). As glucose deprivation reduced the acetylation of GLUD1, we next tested whether GLUD1 deacetylation affected its location. Fig. 5C showed that SIRT3 overexpression promoted the cytoplasmic localization of GLUD1. Similarly, the protein level of $GLUD1^{K84R}$ significantly accumulated in the cytosol compared with $GLUD1^{WT}$ (Fig. 5D). Interestingly, no significant acetylation was observed in GLUD1 isolated from cytosol while GLUD1 isolated from mitochondria was acetylated. (Fig. 5E). These data suggest that GS-induced deacetylation of GLUD1 induces its cytoplasmic localization.

2.6. TRIM21-mediated ubiquitination of GLUD1 enhances cytoplasmic glutamine metabolism

We next tried to clarify the function and regulatory mechanism of cytoplasmic GLUD1 under glucose starvation. Intriguing, overexpressing SIRT3 significantly increased the ubiquitination level of GLUD1, while knockdown SIRT3 decreased its ubiquitination (Fig. 6A–B), and this effect was more obvious under glucose starvation (Fig. 6C). The deacetylation mutant $GLUD1^{K84R}$ also showed increased ubiquitination compared with $GLUD1^{WT}$ (Fig. 6D). We tested the ubiquitination types and found that the K63-linkage ubiquitination of GLUD1 was up-regulated in A549 cells treated with GS (Fig. 6E, Figs. S2A–F). Fig. 6F and G suggested that overexpressing SIRT3 increased the K63-linkage ubiquitination of GLUD1, and the increased ubiquitination of $GLUD1^{K84R}$ was also K63-linkage. However, there was no difference in K48-linkage ubiquitination between $GLUD1^{K84R}$ and $GLUD1^{WT}$ (Fig. 6H). These results demonstrated that the acetylation of GLUD1 affected its K63-linkage ubiquitination.

To find the E3 ligase regulating the K63-linkage ubiquitination of

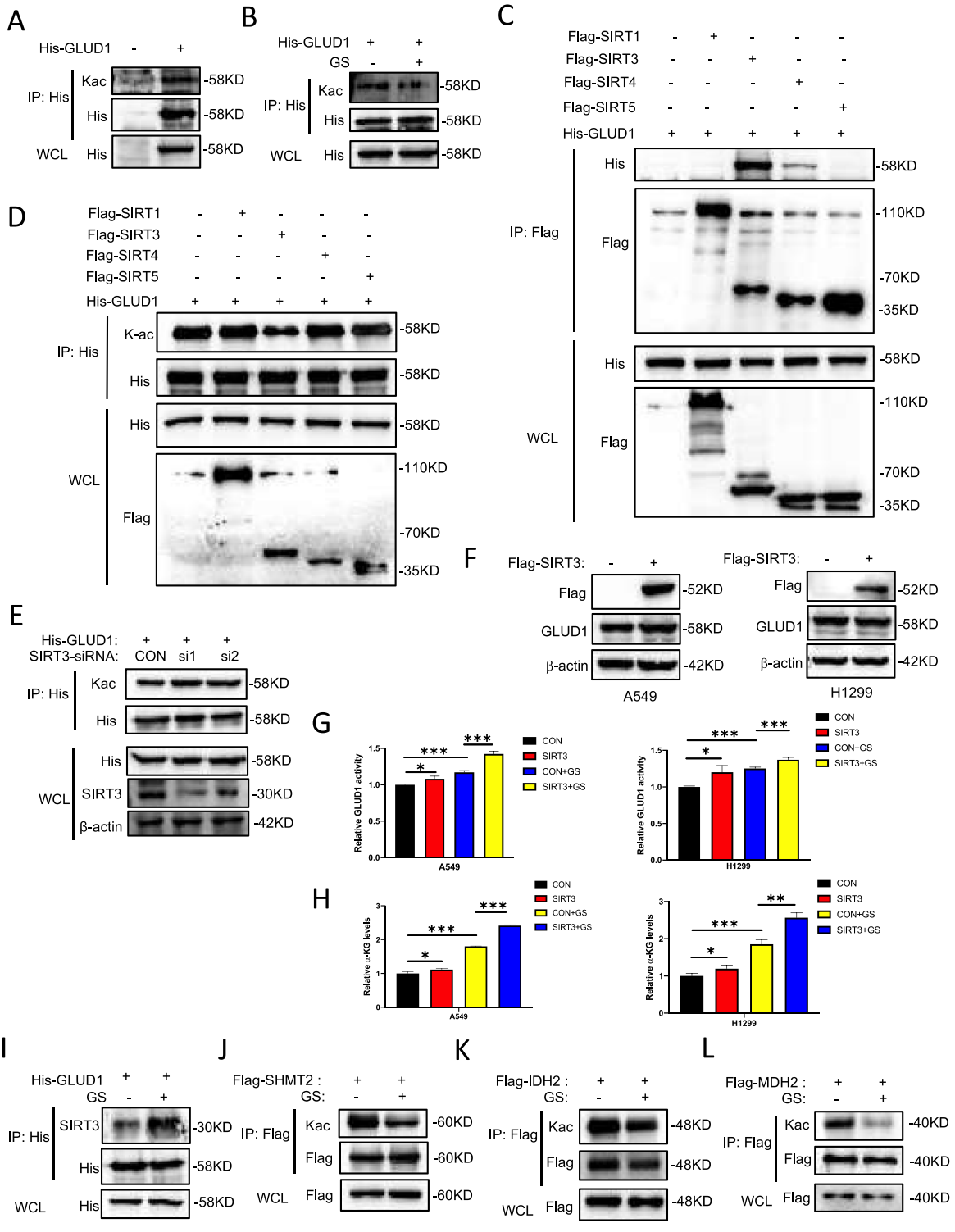

(caption on next page)

Fig. 3. SIRT3 as a deacetylase, impairs the acetylation of GLUD1 and promotes its enzymatic activity. (A) The pcDNA-3.1-His-GLUD1 was transfected into A549 cells, co-IP and Western blot was used to detect the acetylation level of GLUD1. (B) The pcDNA-3.1-His-GLUD1 was transfected into A549 cells with or without GS, co-IP and Western blot was used to detect the acetylation level of GLUD1. (C) A549 cells were transfected with the indicated plasmids, co-IP and Western blot were used to detect the interaction between GLUD1 and SIRT proteins. (D) A549 cells were transfected with these SIRT and GLUD1 plasmids, the acetylation levels of GLUD1 were tested by co-IP and Western blot. (E) In A549 cells, SIRT3 was knockdown to detect the acetylation of GLUD1 using co-IP and Western blot. (F) SIRT3 was overexpressed in A549 (left-hand panel) and H1299 (right-hand panel) cells to detect the level of GLUD1 protein by Western blot. (G) A549 (left-hand panel) and H1299 (right-hand panel) cells were treated with or without GS and overexpressed SIRT3, the activity of GLUD1 was detected by GLUD1 assay kit. Data represent the average of three independent experiments (mean ± SD). $^{*}P < 0.05$, $^{***}P < 0.001$. (H) A549 (left-hand panel) and H1299 (right-hand panel) cells were treated with or without glucose starvation and overexpressed SIRT3, the level of α-KG was detected by α-KG assay kit. Data represent the average of three independent experiments (mean ± SD). $^{*}P < 0.05$, $^{**}P < 0.01$, $^{***}P < 0.001$. (I) His-GLUD1 plasmids was transfected into A549 cells with or without GS. Co-IP and Western blot were used to detect the binding between GLUD1 and SIRT3. (J–L) pCMV-Flag-SHMT2 (J), pCMV-Flag-IDH2 (K) or pCMV-Flag-MDH2 (L) plasmids was transfected into A549 cells with or without GS. Co-IP and Western blot were used to detect the acetylation of indicated proteins.

GLUD1, we performed mass spectrometry analysis and identified the E3 ligases TRIM21, TRIM25 and MKRN2 as putative GLUD1-interacting proteins (Fig. S2G). We found that overexpressing TRIM21 increased the ubiquitination of GLUD1, while TRIM21 knockdown decreased its ubiquitination (Fig. 6I and J). However, TRIM25 and MKRN2 did not affect the ubiquitination of GLUD1 (Figs. S2H and I). We then discriminated the ubiquitin chain types of GLUD1 induced by TRIM21. Our results indicated that overexpressing TRIM21 up-regulated the K63-linkage ubiquitination of GLUD1 (Fig. 6K), but not K48-linkage ubiquitination (Fig. 6L). We next verified the interaction between TRIM21 and GLUD1 in A549 cells. Fig. 6M and N showed that TRIM21 interacted with GLUD1 and this interaction could be further enhanced under glucose starvation (Fig. 6O). Furthermore, TRIM21 showed a stronger binding ability with $GLUD1^{K84R}$ than $GLUD1^{WT}$ (Fig. 6P). These results indicate that deacetylation of GLUD1 promotes TRIM21-mediated ubiquitination.

We next tried to explore the functions of the GLUD1 ubiquitination mediated by TRIM21. As ubiquitination could regulate protein stability, we first examined the protein expression of GLUD1 when overexpressing TRIM21. The results showed that overexpressing TRIM21 did not affect the expression of GLUD1 protein in A549 and H1299 cells (Figs. S3A and B). These results were not surprising as Lys63-linkage ubiquitination always modulated non-degradative processes. In cancer cells, glutamine catabolism occurs both in mitochondria and cytoplasm. As another key enzyme in glutamine catabolism, the kidney-type glutaminase has two subtypes: the shorter isoform GAC located mainly in mitochondria and the longer isoform KGA located in cytoplasm. Interestingly, we discovered that TRIM21 promoted the interaction between GLUD1 and KGA, indicating that TRIM21 might enhance the cytoplasmic glutamine metabolism (Fig. 6Q). Under glucose starvation, GLUD1 bound more KGA in the cytoplasm (Fig. 6R). Overexpressing SIRT3 also significantly increased the interaction between GLUD1 and KGA (Fig. 6S), and the deacetylation mutant $GLUD1^{K84R}$ showed a stronger interaction with KGA than wild-type GLUD1 (Fig. 6T), suggesting that GLUD1 deacetylation induced by glucose starvation promoted the formation of GLUD1-KGA complex, thus enhancing cytoplasmic glutamine catabolism. Taken together, these data elucidate that TRIM21-mediated K63-linkage ubiquitination promotes the cytoplasmic glutamine metabolism by enhancing the interaction between GLUD1 and KGA under glucose starvation.

2.7. GLUD1 reduces p62 body formation by inhibiting the acetylation of p62

SQSTM1/p62 plays a key role in autophagy, which delivers the target proteins to the lysosome by direct binding (Kwon & Ciechanover, 2017). We discovered that GLUD1 could interact with p62 in A549 cells (Fig. 7A and B), and p62 colocalized with GLUD1 in A549 cells tested by immunofluorescence (Fig. 7C). Moreover, glucose starvation enhanced the binding of GLUD1 with p62 (Fig. 7D). The $GLUD1^{K84R}$ mutant also bound more p62 than $GLUD1^{WT}$ (Fig. 7E). These data suggested that the deacetylation of GLUD1 promoted its interaction with p62. P62 bodies have been observed in cells under glucose starvation (Pankiv et al., 2007), they localize to autophagosome formation sites and assemble via self-oligomerization. We found that glucose starvation promoted p62 body formation in A549 cells (Fig. 7F). GLUD1 knockout significantly increased p62 bodies, suggesting that GLUD1 inhibited p62 body formation (Fig. 7G). Previous study demonstrated that acetylation was an important post-translational modification of p62 to form p62 bodies (You et al., 2019). We then tested the acetylation of p62 in A549 cells with GLUD1 knockout and A549 wild-type cells. Fig. 7H showed that GLUD1 knockout promoted the acetylation of p62. HDAC6 was demonstrated to be the key deacetylase of p62. We also found that GLUD1 promoted the binding of p62 with HADC6, thus decreasing the acetylation of p62 (Fig. 7I). Collectively, the data demonstrate that GS-induced cytoplasmic GLUD1 can also regulate autophagy by directly binding to p62 and blocking the formation of p62 bodies, except for acting as a metabolic enzyme to produce α-KG for autophagy inhibition. To further examine whether the acetylation level of GLUD1 affected the proliferation of LUAD cells, we established $GLUD1^{WT}$ and $GLUD1^{K84R}$-A549 cell lines (Fig. 7J). The xenograft assay was performed to determine the effects of $GLUD1^{WT}$-A549 cells and $GLUD1^{K84R}$-A549 mutant cells on tumor growth. Our data indicated that $GLUD1^{K84R}$-A549 cells further enhanced tumorigenicity compared with $GLUD1^{WT}$-A549 cells (Fig. 7K), and $GLUD1^{K84R}$-A549 cells showed an increase in tumor size and weight compared with $GLUD1^{WT}$-A549 cells (Fig. 7L and M).

Taken together, this study reveals a new role of GLUD1 in maintaining cancer cell survival under glucose deprivation. When cancer cells suffer from glucose starvation, GLUD1 is deacetylated by SIRT3. This promotes the formation of GLUD1 hexamer and increases its activity. Besides, the deacetylation induces the cytoplasmic localization of GLUD1. TRIM21 ubiquitinates GLUD1 in K63-linkage, leading to the formation of GLUD1-KGA complex and activation of cytoplasmic glutamine metabolism. These effects enhance glutamine metabolism both in mitochondria and cytoplasm, increase the production of a-KG, thus blocking autophagic cell death. What's more, cytoplasmic GLUD1 can also interact with p62 and prevent its acetylation, leading to the inhibition of p62 body formation. All these effects inhibit autophagic cell death induced by glucose starvation (Fig. 7N).

3. Discussion

Due to the rapid nutrient consumption of cancer cells and poor vascularization in solid tumors, cancer cells often suffered from glucose starvation (Sullivan et al., 2019). In order to adapt to the harsh environment, cancer cells exhibit metabolic flexibility (alternative materials and energy sources). Under glucose deprivation situations, cancer cells can utilize other nutrients to fulfill metabolic needs, such as glutamine, fatty acids, lactate and branched-chain amino acids (Faubert et al., 2017; Hui et al., 2017; Sivanand & Vander Heiden, 2020; Son et al., 2013; Yang et al., 2014). Glutamine catabolism has emerged as a crucial metabolic node in rapidly proliferating cancer cells. However, the functions of glutamine catabolism under glucose deprivation have been less studied. In this study, we discovered a new role of GLUD1, one of the key enzymes in glutamine catabolism, under glucose deprivation. On one hand, glucose deprivation increased GLUD1 activity, producing α-KG to block autophagy. On the other hand, the GS-induced cytoplasmic GLUD1 interacted with p62, inhibiting the formation of p62 bodies. This led to

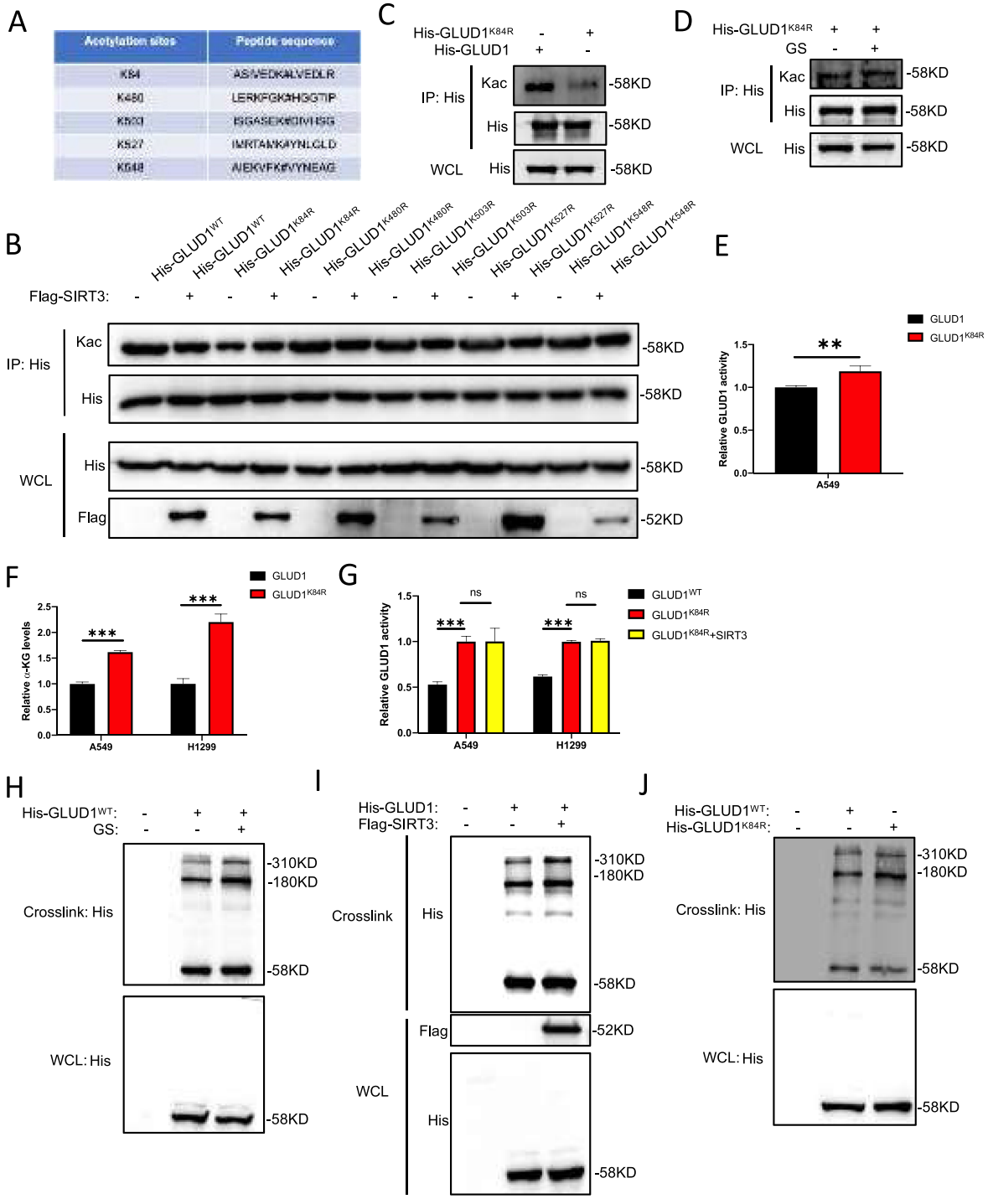

Fig. 4. The K84-acetylation of GLUD1 affect its protein activity and hexamer formation. (A) The acetylation sites of GLUD1 predicted by PhosphoSitePlus. (B and C) The GLUD1 lysine residue mutation plasmids (lysine to arginine) are constructed based on the predicted acetyl sites of GLUD1. A549 cells were transfected with the indicated plasmids, the acetylation levels of GLUD1 were tested by co-IP and Western blot. (D) Overexpression pcDNA-3.1-His-GLUD1^{K84R} in A549 cells were treated with or without GS, co-IP and Western blot was used to detect the acetylation level of GLUD1^{K84R}. (E) The activity of GLUD1^{WT} and GLUD1^{K84R} in A549 cells was detected by GLUD1 activity assay kit. Data represent the average of three independent experiments (mean ± SD). $^{**}P < 0.01$. (F) Overexpression pcDNA-3.1-His-GLUD1^{WT} or pcDNA-3.1-His-GLUD1^{K84R} in A549 and H1299 cells, the level of α-KG was detected via α-KG assay kit. (G) His-GLUD1^{K84R} and Flag-SIRT3 were transfected into A549 and H1299 cells, at the indicate time, His-GLUD1^{K84R} protein was purified by immunoprecipitation. The GLUD1 activity was measured by GLUD1 activity assay kit. Data represent the average of three independent experiments (mean ± SD). ns: $P > 0.05$, $^{***}P < 0.001$. (H) Cell lysates of A549 cells treated with GS and expressed His-GLUD1^{WT} were added with or without 0.025% glutaraldehyde and analyzed through Western blot with anti-His antibody. (I) Cell lysates of A549 cells expressing His-GLUD1 and Flag-SIRT3 were treated with or without 0.025% glutaraldehyde and analyzed by Western blot with anti-His antibody. (J) Cell lysates of A549 cells expressing His-GLUD1^{WT} or His-GLUD1^{K84R} were added with or without 0.025% glutaraldehyde and analyzed through Western blot with anti-His antibody.

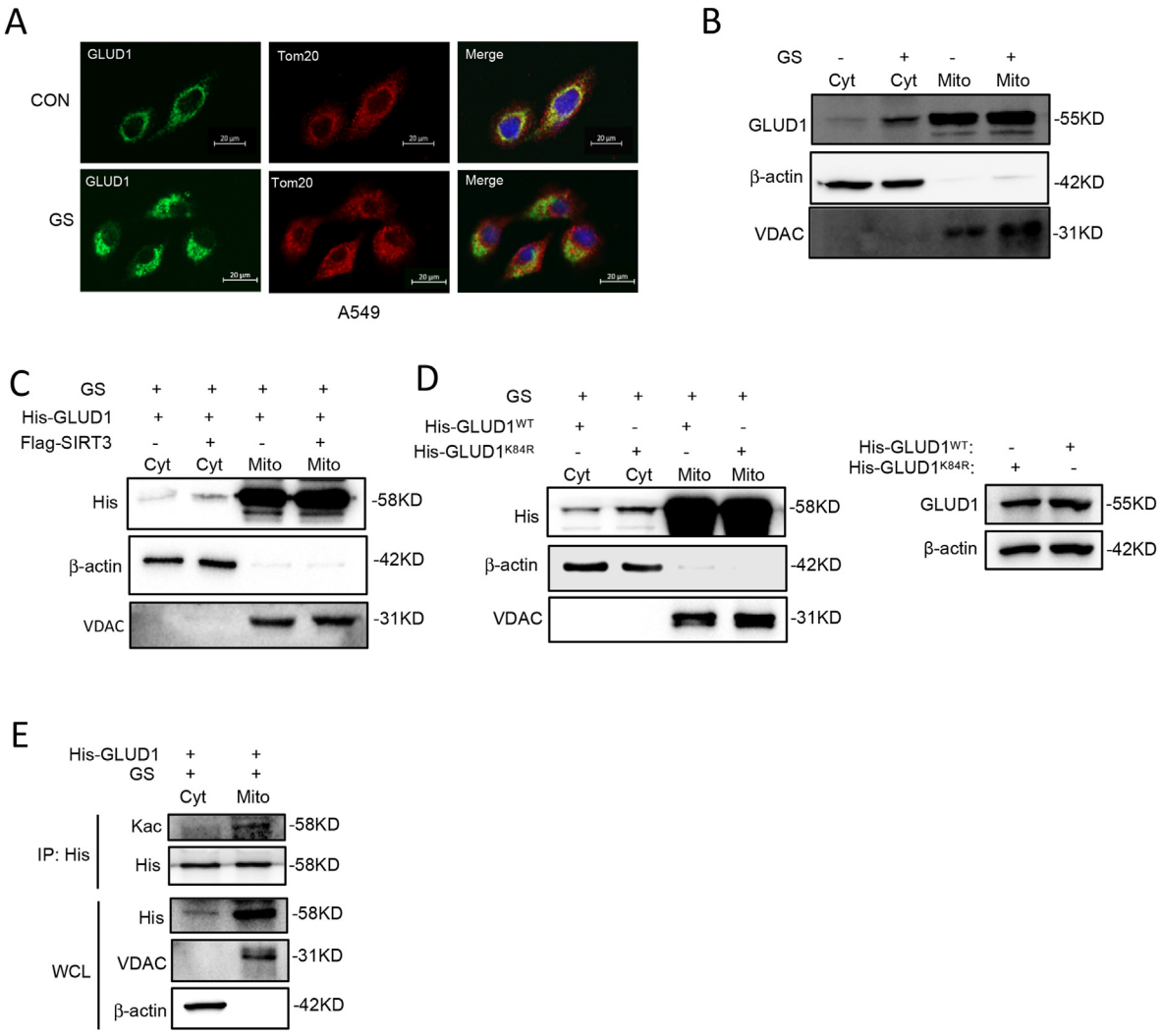

Fig. 5. The glucose starvation induces GLUD1 translocation to cytoplasm

(A and B) In A549 cells with or without GS, the subcellular location of GLUD1 was indicated by immunofluorescence (A) and mitochondria isolation kit (B) followed by Western blot. Scale bars: 20 μm. (C) The His-GLUD1 and Flag-SIRT3 was transfected in A549 cells were treated with GS. The subcellular location of GLUD1 was performed via mitochondria isolation assay and Western blot. (D) The His-GLUD1^{WT} or His-GLUD1^{K84R} was transfected into A549 cells were treated with GS. The subcellular location of GLUD1 was performed via mitochondria isolation assay and Western blot (left-hand panel). The protein level of GLUD1 in WCL was shown (right-hand panel). (E) The His-GLUD was transfected into A549 cells under GS. The acetylation levels of GLUD1 in mitochondria and cytoplasm were detected by mitochondria isolation assay, co-IP and Western blot.

autophagy inhibition and maintained survival of LUAD cells under glucose deprivation. Previous study showed that activation of glutaminolysis by leucine and glutamine promoted cell growth under amino acid deprivation condition in an mTORC1-dependent manner (Duran et al., 2012). Interestingly, another study found that GLUD1 degradation sustained the survival of kidney renal clear cell carcinoma (KIRC) cells via restricting protein synthesis under amino acid deprivation (Shao et al., 2021). These study together with ours suggest that GLUD1 may play various roles in different tumor types or different nutritional conditions.

Autophagy is a double-edged sword during cancer progression. Autophagy can improve the tolerance of tumor cells to harmful stress and maintain survival under nutrient deprivation, while excessive autophagy induces autophagic cell death and inhibits tumor development. Previous study showed that GLUD1 modulated autophagy through a dual mechanism: one was activating mTORC1, the other was limiting the formation of ROS. It is worth noting that these studies were conducted under amino acid deprivation (Duran et al., 2012; Lorin et al., 2013). However, the functions and mechanisms of GLUD1 in glucose starvation-induced autophagy were still less known. Our study demonstrated that GLUD1 protected LUAD cells from autophagic cell death under glucose deprivation. This function was also achieved by a dual mechanism: the enzymatic and non-enzymatic modes. In the enzymatic mode, glucose starvation increased GLUD1 activity, leading to enhanced glutamine metabolism both in mitochondria and cytoplasm. In non-enzymatic mode, cytoplasmic GLUD1 induced glucose starvation interacted with p62, decreasing the acetylation of p62 and inhibiting the formation of p62 bodies. In our previously published paper, we have demonstrated that GLUD1 was overexpressed in LUAD cells than human bronchial epithelial cell (Hu et al., 2023b). Together with this work, our studies can explain why tumor cells have better survival abilities under glucose deficient environment.

Lysine acetylation is an important post-translational modification, which regulates many life activities such as signal transduction and cell metabolism by affecting the stability or activity of proteins. In mitochondria, SIRT3 is the major NAD^+-dependent deacetylase, which has been extensively studied in tumorigenesis (Wei et al., 2018). Some researchers showed that SIRT3 functioned as a tumor suppressor in gastric cancer and hepatocellular carcinoma, while SIRT3 was also reported to act as an oncogene in lung cancer, bladder cancer and breast cancer

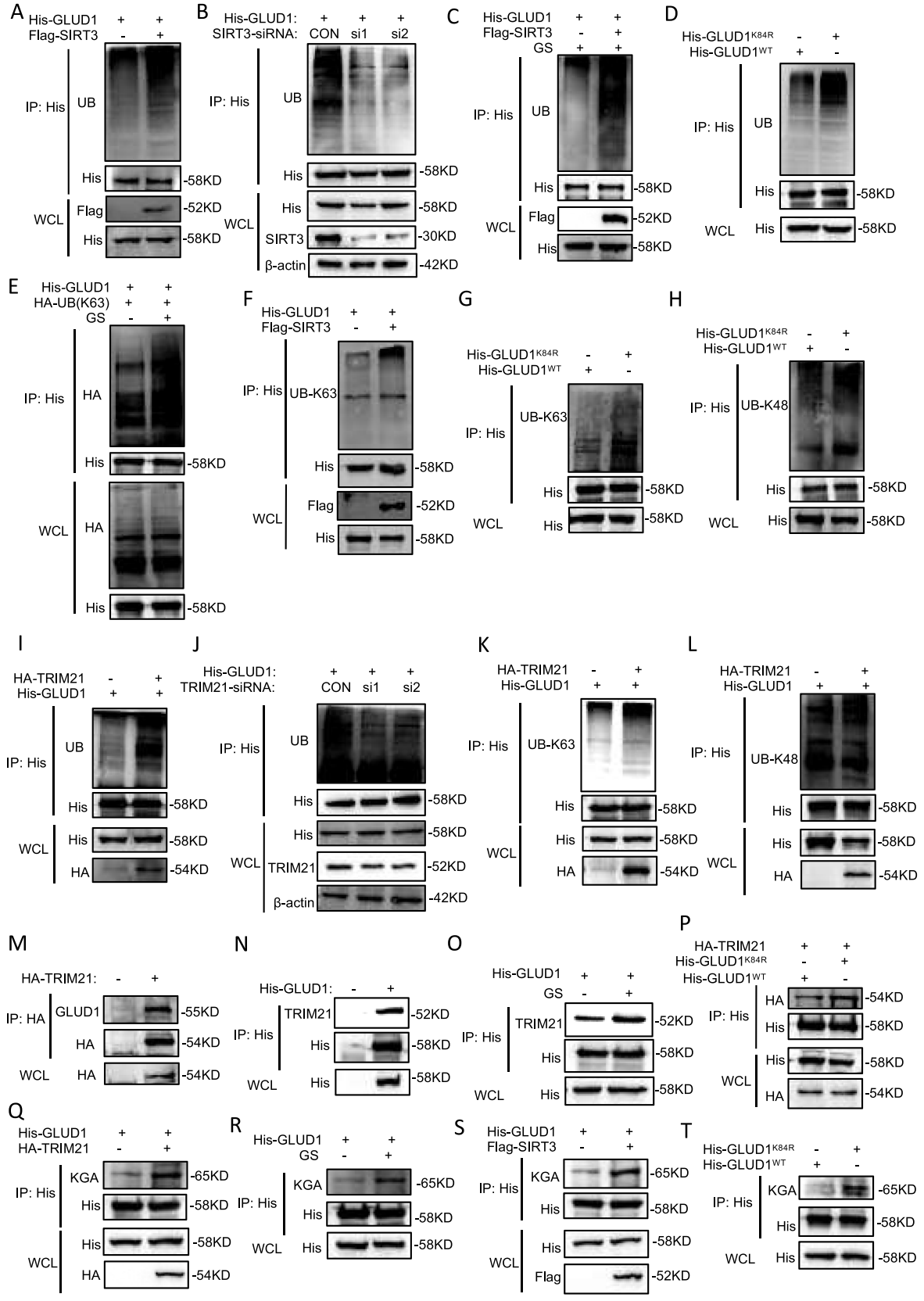

(caption on next page)

Fig. 6. TRIM21-mediated ubiquitination of GLUD1 promotes the formation of GLUD1-KGA complex. (A) The His-GLUD1 and Flag-SIRT3 were transfected into A549 cells, co-IP and Western blot was used to detect the ubiquitination level of GLUD1. (B) The His-GLUD1 and SIRT3-siRNAs were transfected into A549 cells, co-IP and Western blot was used to detect the ubiquitination level of GLUD1. (C) The His-GLUD1 and Flag-SIRT3 were transfected into A549 cells under GS, the ubiquitination level of GLUD1 was tested via co-IP and Western blot. (D) The His-GLUD1^{WT} and His-GLUD1^{K84R} were transfected into A549 cells, co-IP and Western blot was used to detect the ubiquitination level of GLUD1. (E) The His-GLUD1 and HA-UB(K63) were transfected into A549 cells under GS, the K63-ubiquitination level of GLUD1 was tested via co-IP and Western blot. (F) A549 cells were transfected with the indicated plasmids. The K63-ubiquitination of GLUD1 protein was detected by co-IP and Western blot. (G and H) A549 cells were transfected with the indicated plasmids. The K63-ubiquitination (G) and K48-ubiquitination (H) of GLUD1 protein was detected by co-IP and Western blot. (I) The His-GLUD1 and HA-TRIM21 were transfected into A549 cells, co-IP and Western blot was used to detect the ubiquitination level of GLUD1. (J) In A549 cells overexpression GLUD1, TRIM21 was knockdown to detect the ubiquitination of GLUD1 using co-IP and Western blot. (K and L) A549 cells were transfected with the indicated plasmids. The K63-ubiquitination (K) and K48-ubiquitination (L) of GLUD1 protein was detected by co-IP and Western blot. (M and N) A549 cells were transfected with the indicated plasmids, co-IP and Western blot were used to detect the interaction between GLUD1 and TRIM21. (O) The His-GLUD1 were transfected into A549 cells and treated with or without GS, co-IP and Western blot were used to detect the interaction between GLUD1 and TRIM21. (P) The GLUD1^{K84R} binding more TRIM21 than GLUD1^{WT}. Co-IP and Western blot were used to detect the interaction between GLUD1 and TRIM21. (Q) A549 cells were transfected with the indicated plasmids, co-IP and Western blot were used to detect the interaction between GLUD1 and KGA. (R) The His-GLUD1 were transfected into A549 cells with or without GS, co-IP and Western blot were used to detect the interaction between GLUD1 and KGA. (S) A549 cells were transfected with the indicated plasmids, co-IP and Western blot were used to detect the interaction between GLUD1 and KGA. (T) Indicated plasmids was transfect to A549 cells, co-IP and Western blot were used to detect the interaction between GLUD1 and KGA.

(Ansari et al., 2017). These suggested that SIRT3 might play different roles in different tumors according to its regulatory substrates. Although some studies have reported that SIRT3 regulated GLUD1 activity, the exact molecular mechanism was still unclear (Hu et al., 2023c; Li et al., 2019). In our study, we found that SIRT3 was the main deacetylase of GLUD1, and this deacetylation improved GLUD1 activity by promoting GLUD1 hexamer formation. We also elucidated K84 was the key acetylation site of GLUD1 under glucose deprivation. Interestingly, this site was different from the previously reported acetylation site (K503) in colon cancer. In fact, our previous study has demonstrated that K503 of GLUD1 was the key ubiquitination site in LUAD cells. Thus, the modification on the same site of GLUD1 in different types of tumors may be different. This also makes it necessary to study the same modification of proteins in different tumors. We further found that SIRT3 up-regulated the K63-linkage ubiquitination of GLUD1 by promoting the interaction between GLUD1 and TRIM21. TRIM21 is well known to be involved in cancer, inflammation and autoimmunity (Alomari, 2021). TRIM21 regulates tumorigenesis by affecting the activity and stability of target proteins, such as p53, NF-κB and BCL2 (Jauharoh et al., 2012; Reddy et al., 2014; Wada et al., 2009). However, studies focused on the effects of TRIM21 on metabolic enzymes were relatively less. Our study discovered that TRIM21 could ubiquitinate GLUD1 though K63-linkage and promote the formation of GLUD1-KGA complex, thus increasing its enzymatic activity in cytoplasm. This further deepens people's understanding of TRIM21 in cancer.

In conclusion, our study discovers a new function of GLUD1 under glucose deprivation in LUAD cells and clarifies its regulatory mechanism in this condition. This provides new insights into the functions of metabolic reprogramming during cancer progression and lays theoretical basis for the development of anti-tumor drugs.

4. Materials and methods

4.1. Antibodies and regents

Antibodies: The mouse monoclonal antibody against His tag (MA1-21315, 1:5000), HA (26183, 1:3000) and ubiquitin (14-6078-82, 1:1000) were purchased from Thermo Fisher Scientific. The mouse monoclonal antibody against β-actin (60008-1-Ig, 1:4000), Flag tag (66008-4-Ig, 1:3000), GLUD1 (67026-1-Ig, 1:3000) and VDAC1 (66345-1-Ig, 1:2000); The rabbit polyclonal antibody against KGA (20170-1-AP), SIRT3 (10099-1-AP, 1:1000), AMPK (10929-2-AP, 1:1000), Beclin1 (11306-1-AP, 1:2000), ULK1(20986-1-AP, 1:1000), GLUD1(14299-1-AP, 1:2000), GAC (12855-1-AP, 1:2000) and LC3B (18725-1-AP, 1:1000) were ordered from Proteintech. The rabbit polyclonal antibody against P-AMPK (2535T, 1:1000), K63-linkage-specific polyubiquitin antibody (5621, 1:1000) and K48-linkage-specific polyubiquitin antibody (8081, 1:1000) were obtained from Cell Signaling Technology. The mouse monoclonal antibody against SQSTM1/p62 monoclonal antibody (TA502127,1:2000); The rabbit polyclonal antibody against P-ULK1 (TA383093, 1:1000) were ordered from OriGene. The anti-Acetyllysine mouse mAb (PTM-101, 1:1000) were ordered from PTM BIO.

Reagents: Chloroquine (C7698) were ordered from Sigma. Four percent polyformaldehyde (P1110) was purchased from Solarbio. H2DCFDA (HY-D0940) was purchased from MCE. Enhanced mitochondrial membrane potential assay kit with JC-1 (C2003S) was purchased from Beyotime. GLUD1 siRNAs (AM16708) and Beclin1 siRNAs (AM16708) were ordered from Thermo Fisher.

4.2. Plasmids

PCR-amplified GLUD1, TRIM21 and p62 were cloned into pcDNA-His/v5, pCDH-Flag, pCMV-HA vectors. GLUD1(K84R), GLUD1(K480R), GLUD1(K503R), GLUD1(K527R) and GLUD1(K548R) mutations plasmids were generated using the ClonExpress II One Step Cloning kit (Vazyme). Overexpressing SIRT7 plasmids were donated by Professor Hongquan Zhang. The primer sequences are shown in Table S1. Overexpressing TRIM25 and MKRN2 were obtained from MiaoLingBio, China.

4.3. Cell culture

Lung adenocarcinoma cell lines A549 (1101HUM-PUMC000002) and H1299 (1101HUM-PUMC000469) were purchased from the National Collection of Authenticated Cell Clutures and cultured in RPMI 1640 supplemented with 10% FBS (SORFA). All cells were cultured under an atmosphere of 5% CO_2 at 37 °C.

4.4. Transfection

Cells were seeded in plates and reached a density of 70%–80%, indicated plasmids or siRNAs were transfected using SuperFectin DNA Transfection Reagent kit (Pufei, 2102–100) or siTran 2.0 siRNA transfection reagent (OriGene, TT320002) according to the manu-facturer instructions.

4.5. CRISPR-Cas9-mediated knockout of GLUD1

Stable knockout of GLUD1 in A549 cells was achieved using a CRISPR-Cas9 system. Lentiviral plasmids were transfected into HEK293T cells together with pSPAX2 and pMD.2G using SuperFectin DNA Transfection Reagent kit. After 48 h, lentiviral supernatants were harvested and infected A549 cells with 5 μg/mL of polybrene (SANTA CRUZ, sc-134220). Uninfected cells were killed by 4 μg/mL purinomycin (Solarbio, P8230) for 3 days.

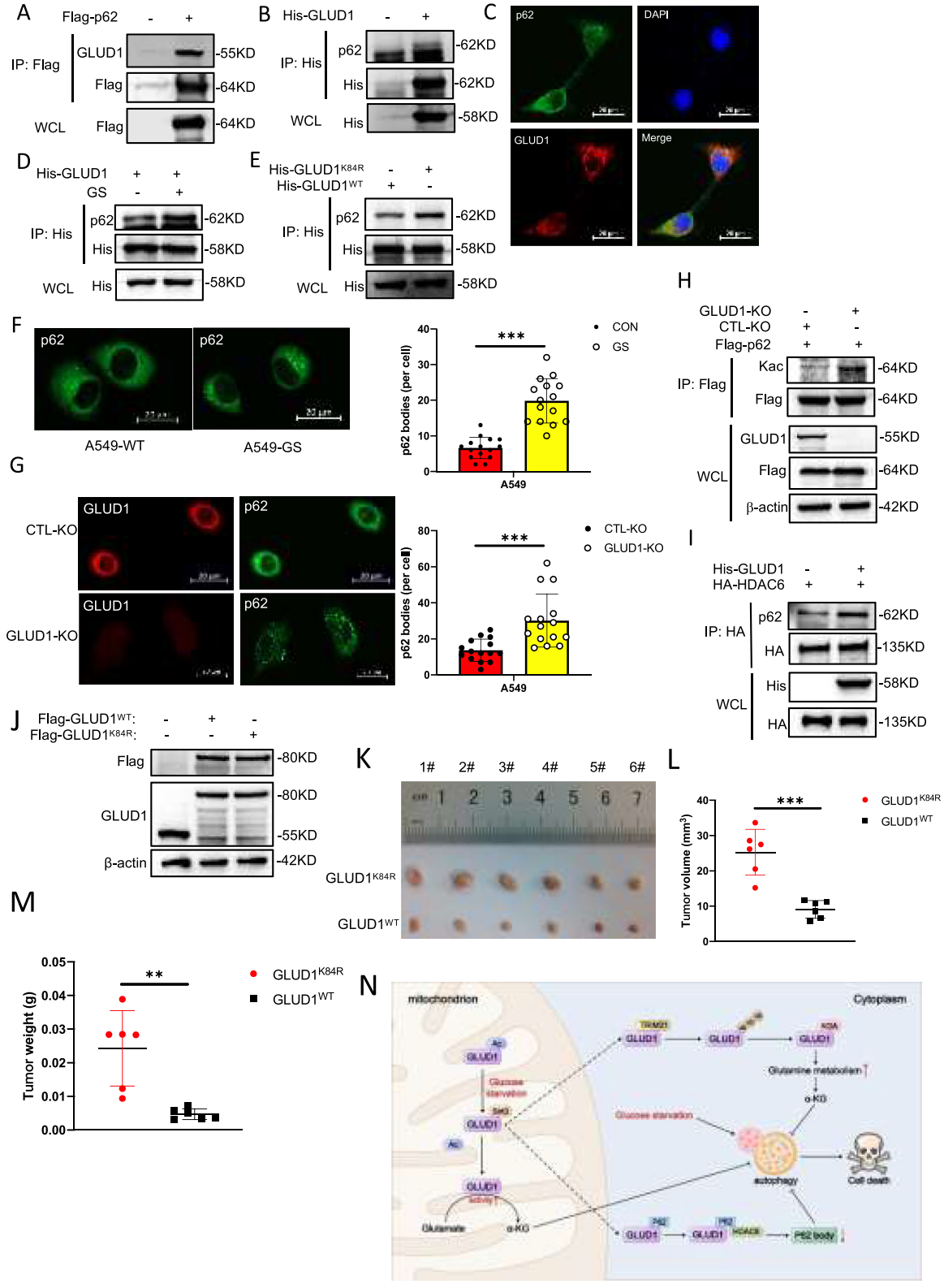

(caption on next page)

Fig. 7. GLUD1 reduces p62 bodies formation by inhibiting the acetylation of p62. (A and B) A549 cells were transfected with the indicated plasmids, co-IP and Western blot were used to detect the interaction between GLUD1 and p62. (C) The colocalization of GLUD1 and p62 was detected by immunofluorescence with GLUD1 and p62 antibodies. (D) A549 cells were transfected with His-GLUD1 under GS, co-IP and Western blot were used to detect the interaction between GLUD1 and p62. (E) A549 cells were transfected with His-GLUD1^{WT} or His-GLUD1^{K84R}, the binding between GLUD1 and p62 was detected by co-IP and Western blot. (F) P62 bodies was observed in A549 cells with or without GS by immunofluorescence with p62 antibodies (left-hand panel). Scale bars, 20 μm. Quantification of p62 bodies (right-hand panel). The data are presented as mean ± SD, $n = 15$ cells. ***$P < 0.001$. (G) Knockout GLUD1 affects the formation of p62 bodies in A549 cells. P62 bodies was observed by immunofluorescence with GLUD1 and p62 antibodies (left-hand panel). Scale bars, 20 μm. Quantification of p62 bodies (right-hand panel). The data are presented as mean ± SD, $n = 15$ cells. ***$P < 0.001$. (H) The acetylation of p62 in GLUD1-KO and control A549 cells was detected by co-IP and Western blot. (I) A549 cells were transfected with the indicated plasmids, co-IP and Western blot were used to detect the interaction between HDAC6 and p62. (J) GLUD1-KO-A549 cell lines were constructed by CRISPR-Cas9, Flag-GLUD1^{WT} or Flag-GLUD1^{K84R} plasmid were transfected in GLUD1-KO-A549 cell lines. The expression of the GLUD1 protein was detected by western blotting. (K–M) GLUD1^{WT}-A549 and GLUD1^{K84R}-A549 cell lines (1×10^7) were subcutaneously injected into the flanks of nude mice (six mice per group). Twenty-eight days later, the tumors were dissected out and photographed (K). The volume (L) and weight (M) of the xenograft tumors were measured. The p value was calculated by paired *t*-test: *$P < 0.05$, **$P < 0.01$. (N) Schematic model of GLUD1 in maintaining cancer cell survival under glucose deprivation.

4.6. Patient-derived lung adenocarcinoma Organoid experiments

The tumor tissues from lung adenocarcinoma patients were washed with cold HBSS. The tissues were cut into small pieces, digested with Tumor Tissue Digestion Solution (BIOGENOUS BIOTECHNOLOGY, INC., Cat No. K601003) and centrifuged to collect the tumor fraction. These tumor fractions were embedded in Matrigel (BD Biosciences, 356231) and seeded on 24-well plates. After matrigel polymerization, culture medium (BIOGENOUS BIOTECHNOLOGY, INC., Cat No. K2138-LA) was added and refreshed every 2 days. For 2-DG (2-Deoxy-D-glucose, MCE, Cat No. HY-13966) and R162 (MCE, Cat No. HY-103096) treatment, the culture medium with 5 mM 2-DG or 20 μM R162 was added and refreshed every 2 days. On day 7, the photographs were taken using Olympus IX71 microscope. All the experiments with human tissue samples were approved and supervised by the Ethics Committee of the First Affiliated Hospital of Nanchang University, with No. (2023) CDYFYYLK (04-003).

4.7. Immunoprecipitation

For immunoprecipitation assay, cells were lysed through NP-40 buffer (150 mM NaCl, 20 mM β-glycerol phosphates, 1 mM Na orthovanadate, 20 mM NaF, 0.5% Nonidet P-40, 20 mM Hepes, pH 7.4) added with PMSF for 30 min at 4 °C. Then the lysates were added Protein G-Agarose (Roche, 11243233001) and the indicated antibodies incubate overnight at 4 °C. Next, samples were centrifuged 3000*g* for 3 min at 4 °C between each wash. The samples were added with 2 × loading buffer and boiled for 10 min.

4.8. Western blot analysis

Cell lysates were added to 2 × loading buffer and boiled for 10 min. The samples were subjected to 10% SDS-PAGE and then transferred to PVDF membranes (Milipore, IPVH00010). The samples were detected in western blotting with appropriate antibodies.

4.9. Measurement of GLUD1 activity

The GLUD1 activity was measured by Micro Glutamic Acid Dehydrogenase Assay Kit (Beijing Solarbio Science & Technology Co., Ltd). Briefly, cells are cracked using ultrasound. Then 10 μl cells suspension was added in 190 μL Micro Glutamic Acid Dehydrogenase Assay Kit buffer 1. 20 s later, the absorbance at 340 nm was measured by Microplate Reader (A_1). After 5 min 20 s, the absorbance at 340 nm was measured again (A_2). $\triangle A=(A_1\text{-}A_2)$ was used for measuring GLUD1 activity.

4.10. Measurement of GLS activity

The GLUD1 activity was measured by Micro Glutaminase (GLS) Assay Kit (Beijing Solarbio Science & Technology Co., Ltd). Briefly, cells were cracked using ultrasound and centrifugate. The 16 μl supernatant was mixed with 64 μL Micro GLS Assay Kit buffer 1 at 37 °C for 1 h. Then, samples were added to another buffers at room temperature for 30 min. The absorbance at 630 nm was measured by Microplate Reader.

4.11. Measurement of α-KG content in cells

Cells were lysed with RIPA buffer (SEVEN, SW104-02) containing protease inhibitors, and centrifuged at 12000*g* for 10 min at 4 °C. Then, the 20 μL lysates were used for detection in 180 μL assay solution (100 mM KH_2PO_4 [Solarbio, P7392], pH 7.2, 10 mM NH_4Cl [Solarbio, A7320], 5 mM $MgCl_2$ [Solarbio, M8161], 0.15 mM NADH, 5 U GLUD1 [Sigma- Aldrich, G2626]) and incubated for 10 min at 37 °C. The absorbance at 630 nm was measured by Microplate Reader. The decreased absorbance was used to detect the level of α-KG.

4.12. Measurement of glutamate content in cells

The glutamate content was measured by Glutamate (Glu) Content Assay Kit (Beijing Solarbio Science & Technology Co., Ltd) according to manufacturer's protocol.

4.13. Measurement of ammonia content in cells

The ammonia content was measured by Blood Ammonia Content Assay Kit (Beijing Solarbio Science & Technology Co., Ltd) according to manufacturer's protocol.

4.14. Immunofluorescence assay

1×10^3 cells were spread in 24-well plate with a cell slide (NEST 801010) and cultured for 24 h. The cell slides were washed with PBS 3 times each 5 min, then 4% paraformaldehyde was added and fixed for 30 min. The cells were washed 3 times with PBS, then sealed with block buffer (3% BSA + 0.2% Trition-X-100 in PBS) 1 h at room temperature, the primary antibodies were incubated overnight. The cells were washed with wash buffer (0.2% BSA + 0.05% Trition-X-100 in PBS) 5 times in 15 min and fluorescent secondary antibodies were incubated for 1 h. The cells were washed 3 times with wash buffer, and then DAPI (Southern Biotech 0100-20) was added to the cells for staining. Finally, the laser confocal microscopy (ZEISS) was used to photograph.

4.15. Mitochondrial and cytoplasmic fractionation

Mitochondria isolation was performed by Qproteome Mitochondria Isolation Kit (QIAGEN 37612) according to manufacturer's protocol.

4.16. Glutaraldehyde crosslink assay

LUAD cells were lysed by NP-40 buffer. The cell lysates were treated with 0.025% glutaraldehyde for 20 min and terminated crosslink by 0.5 M glutamate. Then, the samples were added to 2 × loading buffer and boiled for 10 min. The results analyzed by Western blot.

4.17. Evaluation of cell viability

Cell viability assay was detected with the Cell counting Kit-8 (MCE). 5000 cells in RPMI 1640 with 10% FBS were seeded in 96-well plates, each group cells had three replicates. 24 h later, the cells were treated with GS. At the specified time, cells were added with 10 μL CCK8 and incubated for 1 h at 37 °C. The results were determined by measuring the absorbance at 450 nm.

4.18. Cell proliferation assay

For cell growth assays: 5000 A549 cells were seeded in 24-well plates, each group cells had three replicates. At the specified time, cells were fixed in 4% formaldehyde and staining with 1% crystal violet. Next, cells incubated with 10% acetic acid and the results was determined by measuring the absorbance at 595 nm.

4.19. In vivo xenograft assay

4-week-old male BALB/c-Nude mice were purchased from Gempharmatech Co., Ltd (Jiangsu, China). All nude mice were lived in the SPF animal facility of the Nanchang University and experimental procedures were approved by the Institutional of Nanchang University Approval for Research Involving Animals (NCULAE-20240704001). All animal experiments were performed according to the established guidelines. The study complied with all the relevant ethical regulations on animal research.

GLUD1-depleted A549 cells (1×10^7) rescued with GLUD1-WT or GLUD1-K84R were injected subcutaneously into the flanks of 4-week-old male BALB/C nude mice. After inoculation for 4 weeks, the mice were euthanized, and the tumors dissected out. Tumor volume (calculated as $\pi/6 \times$ [large diameter] $\times$ [smaller diameter]^2) and weight were measured.

4.20. Mass spectrometry analysis

The Mass Spectrometry Analysis was performed and analyzed in PTM BIO (Table S2).

4.21. Statistical analysis

GraphPad Prism 8 software was used for statistical analysis. All data are presented as mean ± SD. Student's *t*-test was used for statistical evaluation, and *P*-values $\leq$0.05 were considered statistically significant.

CRediT authorship contribution statement

Qifan Hu: Writing – original draft. **Longhua Sun:** Supervision. **Zhujun Cheng:** Writing – review & editing. **Lei Wang:** Data curation, Conceptualization. **Xiaorui Wan:** Data curation. **Jing Xu:** Data curation. **Junyao Cheng:** Data curation. **Zuorui Wang:** Data curation. **Yi Yuan:** Formal analysis, Data curation. **Keru Wang:** Data curation. **Tianyu Han:** Writing – review & editing, Funding acquisition.

Declaration of competing interest

The authors declare that they have no conflicts of interest with the contents of this article.

Acknowledgements

This work was supported by the National Natural Science Foundation of China (82273258, 81902346, 82360474), Natural Science Foundation of Jiangxi Province (20212ACB216007, 20212BAB216030), the Science and Technology Innovation High-end Talent Project of Jiangxi Province (jxsq2023201100), the Training Plan for Academic and Technical Leaders of Major Disciplines in Jiangxi Province (20204BCJ23023), Scientific Research Project of Cultivating Outstanding Young People in First Affiliated Hospital of Nanchang University (YQ202104).

Appendix A. Supplementary data

Supplementary data to this article can be found online at https://doi.org/10.1016/j.cellin.2024.100186.

References

Alomari, M. (2021). TRIM21 - a potential novel therapeutic target in cancer. *Pharmacological Research, 165*, Article 105443. https://doi.org/10.1016/j.phrs.2021.105443

Ansari, A., et al. (2017). Function of the SIRT3 mitochondrial deacetylase in cellular physiology, cancer, and neurodegenerative disease. *Aging Cell, 16*, 4–16. https://doi.org/10.1111/acel.12538

Carrico, C., Meyer, J. G., He, W., Gibson, B. W., & Verdin, E. (2018). The mitochondrial acylome emerges: Proteomics, regulation by sirtuins, and metabolic and disease implications. *Cell Metabolism, 27*, 497–512. https://doi.org/10.1016/j.cmet.2018.01.016

Chu, Z., et al. (2021). FOXO3A-induced LINC00926 suppresses breast tumor growth and metastasis through inhibition of PGK1-mediated Warburg effect. *Molecular Therapy, 29*, 2737–2753. https://doi.org/10.1016/j.ymthe.2021.04.036

Duarte, I. F., et al. (2010). Can nuclear magnetic resonance (NMR) spectroscopy reveal different metabolic signatures for lung tumours? *Virchows Archiv, 457*, 715–725. https://doi.org/10.1007/s00428-010-0993-6

Duran, R. V., et al. (2012). Glutaminolysis activates Rag-mTORC1 signaling. *Molecular Cell, 47*, 349–358. https://doi.org/10.1016/j.molcel.2012.05.043

Faubert, B., et al. (2017). Lactate metabolism in human lung tumors. *Cell, 171*, 358–371 e359. https://doi.org/10.1016/j.cell.2017.09.019

Faubert, B., Solmonson, A., & DeBerardinis, R. J. (2020). Metabolic reprogramming and cancer progression. *Science, 368*. https://doi.org/10.1126/science.aaw5473

Grasmann, G., Smolle, E., Olschewski, H., & Leithner, K. (2019). Gluconeogenesis in cancer cells - repurposing of a starvation-induced metabolic pathway? *Biochimica et Biophysica Acta (BBA) - Reviews on Cancer, 1872*, 24–36. https://doi.org/10.1016/j.bbcan.2019.05.006

Haigis, M. C., et al. (2006). SIRT4 inhibits glutamate dehydrogenase and opposes the effects of calorie restriction in pancreatic beta cells. *Cell, 126*, 941–954. https://doi.org/10.1016/j.cell.2006.06.057

Han, T., et al. (2018). Phosphorylation of glutaminase by PKCepsilon is essential for its enzymatic activity and critically contributes to tumorigenesis. *Cell Research, 28*, 655–669. https://doi.org/10.1038/s41422-018-0021-y

Hanahan, D., & Weinberg, R. A. (2011). Hallmarks of cancer: The next generation. *Cell, 144*, 646–674. https://doi.org/10.1016/j.cell.2011.02.013

Hirayama, A., et al. (2009). Quantitative metabolome profiling of colon and stomach cancer microenvironment by capillary electrophoresis time-of-flight mass spectrometry. *Cancer Research, 69*, 4918–4925. https://doi.org/10.1158/0008-5472.CAN-08-4806

Hirschey, M. D., & Zhao, Y. (2015). Metabolic regulation by lysine malonylation, succinylation, and glutarylation. *Molecular & Cellular Proteomics, 14*, 2308–2315. https://doi.org/10.1074/mcp.R114.046664

Hu, Q., et al. (2023a). Amino acid metabolism regulated by lncRNAs: The propellant behind cancer metabolic reprogramming. *Cell Communication and Signaling, 21*, 87. https://doi.org/10.1186/s12964-023-01116-1

Hu, Q., et al. (2023b). STUB1-mediated ubiquitination regulates the stability of GLUD1 in lung adenocarcinoma. *iScience, 26*, Article 107151. https://doi.org/10.1016/j.isci.2023.107151

Hu, K., et al. (2023c). Glutamate dehydrogenase1 supports HIF-1alpha stability to promote colorectal tumorigenesis under hypoxia. *The EMBO Journal, 42*, Article e112675. https://doi.org/10.15252/embj.2022112675

Hui, S., et al. (2017). Glucose feeds the TCA cycle via circulating lactate. *Nature, 551*, 115–118. https://doi.org/10.1038/nature24057

Jauharoh, S. N., et al. (2012). SS-A/Ro52 promotes apoptosis by regulating Bcl-2 production. *Biochemical and Biophysical Research Communications, 417*, 582–587. https://doi.org/10.1016/j.bbrc.2011.12.010

Kwon, Y. T., & Ciechanover, A. (2017). The ubiquitin code in the ubiquitin-proteasome system and autophagy. *Trends in Biochemical Sciences, 42*, 873–886. https://doi.org/10.1016/j.tibs.2017.09.002

Li, M., et al. (2019). Non-oncogene addiction to SIRT3 plays a critical role in lymphomagenesis. *Cancer Cell, 35*, 916–931 e919. https://doi.org/10.1016/j.ccell.2019.05.002

Liang, X. H., et al. (1999). Induction of autophagy and inhibition of tumorigenesis by beclin 1. *Nature, 402*, 672–676. https://doi.org/10.1038/45257

Liu, X., et al. (2018). Acetate production from glucose and coupling to mitochondrial metabolism in mammals. *Cell, 175*, 502–513 e513. https://doi.org/10.1016/j.cell.2018.08.040

Liu, C. M., et al. (2020). E3 ligase STUB1 attenuates stemness and tumorigenicity of oral carcinoma cells via transglutaminase 2 regulation. *Journal of the Formosan Medical Association, 119*, 1532–1538. https://doi.org/10.1016/j.jfma.2020.06.004

Lorin, S., et al. (2013). Glutamate dehydrogenase contributes to leucine sensing in the regulation of autophagy. *Autophagy, 9*, 850–860. https://doi.org/10.4161/auto.24083

Luan, H., et al. (2018). Loss of the nuclear pool of ubiquitin ligase CHIP/STUB1 in breast cancer unleashes the MZF1-cathepsin pro-oncogenic program. *Cancer Research, 78*, 2524–2535. https://doi.org/10.1158/0008-5472.CAN-16-2140

Pankiv, S., et al. (2007). p62/SQSTM1 binds directly to Atg8/LC3 to facilitate degradation of ubiquitinated protein aggregates by autophagy. *Journal of Biological Chemistry, 282*, 24131–24145. https://doi.org/10.1074/jbc.M702824200

Paul, I., & Ghosh, M. K. (2015). A CHIPotle in physiology and disease. *The International Journal of Biochemistry & Cell Biology, 58*, 37–52. https://doi.org/10.1016/j.biocel.2014.10.027

Reddy, B. A., et al. (2014). Nucleotide biosynthetic enzyme GMP synthase is a TRIM21-controlled relay of p53 stabilization. *Molecular Cell, 53*, 458–470. https://doi.org/10.1016/j.molcel.2013.12.017

Rocha, C. M., et al. (2010). Metabolic profiling of human lung cancer tissue by 1H high resolution magic angle spinning (HRMAS) NMR spectroscopy. *Journal of Proteome Research, 9*, 319–332. https://doi.org/10.1021/pr9006574

Rocha, C. M., et al. (2015). NMR metabolomics of human lung tumours reveals distinct metabolic signatures for adenocarcinoma and squamous cell carcinoma. *Carcinogenesis, 36*, 68–75. https://doi.org/10.1093/carcin/bgu226

Shao, J., et al. (2021). Cytosolic GDH1 degradation restricts protein synthesis to sustain tumor cell survival following amino acid deprivation. *The EMBO Journal, 40*, Article e107480. https://doi.org/10.15252/embj.2020107480

Sivanand, S., & Vander Heiden, M. G. (2020). Emerging roles for branched-chain amino acid metabolism in cancer. *Cancer Cell, 37*, 147–156. https://doi.org/10.1016/j.ccell.2019.12.011

Son, J., et al. (2013). Glutamine supports pancreatic cancer growth through a KRAS-regulated metabolic pathway. *Nature, 496*, 101–105. https://doi.org/10.1038/nature12040

Sullivan, M. R., et al. (2019). Quantification of microenvironmental metabolites in murine cancers reveals determinants of tumor nutrient availability. *Elife, 8*. https://doi.org/10.7554/eLife.44235

Urasaki, Y., Heath, L., & Xu, C. W. (2012). Coupling of glucose deprivation with impaired histone H2B monoubiquitination in tumors. *PLoS One, 7*, Article e36775. https://doi.org/10.1371/journal.pone.0036775

Verdin, E., & Ott, M. (2015). 50 years of protein acetylation: From gene regulation to epigenetics, metabolism and beyond. *Nature Reviews Molecular Cell Biology, 16*, 258–264. https://doi.org/10.1038/nrm3931

Wada, K., Niida, M., Tanaka, M., & Kamitani, T. (2009). Ro52-mediated monoubiquitination of IKKbeta down-regulates NF-kappaB signalling. *Journal of Biochemistry, 146*, 821–832. https://doi.org/10.1093/jb/mvp127

Wang, L., et al. (2013). 1H-NMR based metabonomic profiling of human esophageal cancer tissue. *Molecular Cancer, 12*, 25. https://doi.org/10.1186/1476-4598-12-25

Wei, Z., et al. (2018). Deacetylation of serine hydroxymethyl-transferase 2 by SIRT3 promotes colorectal carcinogenesis. *Nature Communications, 9*, 4468. https://doi.org/10.1038/s41467-018-06812-y

Wei, C., et al. (2021). Tripartite motif-containing protein 6 facilitates growth and migration of breast cancer through degradation of STUB1. *European Journal of Histochemistry, 65*. https://doi.org/10.4081/ejh.2021.3214

Yang, C., et al. (2014). Glutamine oxidation maintains the TCA cycle and cell survival during impaired mitochondrial pyruvate transport. *Molecular Cell, 56*, 414–424. https://doi.org/10.1016/j.molcel.2014.09.025

Yao, K., et al. (2012). Alpha-ketoglutarate inhibits glutamine degradation and enhances protein synthesis in intestinal porcine epithelial cells. *Amino Acids, 42*, 2491–2500. https://doi.org/10.1007/s00726-011-1060-6

You, Z., et al. (2019). Requirement for p62 acetylation in the aggregation of ubiquitylated proteins under nutrient stress. *Nature Communications, 10*, 5792. https://doi.org/10.1038/s41467-019-13718-w

Zhang, S., et al. (2021). Adaptor SH3BGRL promotes breast cancer metastasis through PFN1 degradation by translational STUB1 upregulation. *Oncogene, 40*, 5677–5690. https://doi.org/10.1038/s41388-021-01970-8

Ziebart, T., et al. (2011). Metabolic and proteomic differentials in head and neck squamous cell carcinomas and normal gingival tissue. *Journal of Cancer Research and Clinical Oncology, 137*, 193–199. https://doi.org/10.1007/s00432-010-0875-y